CHAPTER 4

NUMERICAL MODEL

4.1 Preamble

The growing need to understand the complex flow field phenomena involved in gas turbine combustors has led to the development of fundamentally based analytical approaches to assist the design process. CFD forms a major category of such procedures and is a key component in the present and future development of combustors. The detailed information obtained from numerical simulations is needed to analyze stresses and thermal conditions in the metal parts of the flame tube. The thermal and flow conditions at the exit of the combustor also greatly influence numerical simulations of heat transfer to the turbine blades and discs. This chapter describes the fundamentals of a CFD model that was developed using a commercial code. An investigation of the different combustion models available, i.e. kinetically controlled reaction model, turbulence-controlled eddy break-up model, hybrid kinetics/eddy break-up model, combined time scale model and a presumed-PDF model of unpremixed turbulent reaction, led to the implementation of the PPDF combustion model to numerically model the research combustor. A short description of the PPDF-model implemented by the numerical code is given. The computational grid used to model the external and internal flow field is described as well as the boundary values used. The computational model was not developed by the author but only implemented and modified to correspond to the correct test conditions. The relevant information that describes the numerical model is obtained from the corresponding references [33-37].

4.2 Presumed-PDF model of unpremixed turbulent reaction

The Presumed-PDF model implemented [38] was developed by the combustion community to predict unpremixed or diffusion flames formed at the interface between separately-introduced fuel-bearing and oxidant-bearing streams. This model employs the fast-kinetics assumption, which results in turbulent mixing between the streams being the rate-controlling process. The particular model incorporated in the commercial code characterizes the mixing process in terms of:

- The time-average fields of the mixture fraction f and its mean square fluctuations or 'variance' g_f, defined as

$$g_f \equiv \overline{f'^2} \tag{4.1}$$

  where f' is the instantaneous fluctuation about the mean and the overbar denotes the time average. Each field is governed by its own differential transport equation.
- A presumed form of probability density function (pdf) for the instantaneous mixture fraction $\hat{f}$, which depends on the above mentioned variables and is denoted by P(f).

Under certain circumstances, to be described below, the instantaneous temperature $\hat{T}$, density ρ and species concentration $\hat{m}$ can each be uniquely related to $\hat{f}$. Their time-average values can then be determined from

$$\phi = \int_0^1 \hat{\phi}(f)P(f)df \tag{4.2}$$

where $\hat{\phi}$ stands for any of the aforementioned variables. Thus the complete model consists of the transport equations for f and g_f, the presumed pdf, P(f), and the set of

$\hat{\phi}(f)$ relations for $\hat{T}$, $\hat{m}_i$ and ρ. The $\hat{\phi}(f)$ functions are derived from the particular assumptions made about the instantaneous reactions and are specific to each fuel/oxidant combination. The principle assumptions are:

- the reactions are fast, leading to thin burning zones embedded in the turbulent flow field;
- the thermochemical state at any point within such a zone is uniquely related to $\hat{f}$.

The second assumption strictly requires that the zone be adiabatic, although empirical means of correcting for heat losses have been devised. The fast reaction assumption allows some degree of freedom in the reaction representation, the main practices being as follows:

- 'Mixed as burnt' models, which assume a single-step irreversible reaction and enable the $\hat{\phi}(f)$ to be determined straightforwardly from the stoichiometry and thermophysical properties.
- 'Equilibrium' models, which can encompass the full reaction mechanism but assume that all reactions reach equilibrium, i.e. forward and backward rates are equal. For these, the $\hat{\phi}(f)$ have to be determined using the appropriate equilibrium and thermophysical data and a solution scheme for the associated simultaneous non-linear algebraic equations.
- 'Laminar flamelet' models, which presume that the reactions take place at finite rates in one-dimensional transient laminar flames. Here, the determination of the $\hat{\phi}(f)$ involves solution of the unsteady one-dimensional mass, momentum, energy and species concentration equations for the laminar flame.

4.3 Computational grid

A close look at the combustor reveals the existence of a geometric symmetry plane. In order to reduce the computational effort, it was therefore decided to split the combustor along the symmetry (or cyclic) plane and model only one half of the combustor. The computational grid was generated in three stages. During the first stage the computational grid for the flow field inside the combustor was generated. During the second stage the computational grid for the combustor liner was generated. This was accomplished by adding an extra layer of cells on the outer surface of the flow domain by extrusion of a set of boundary shells which were generated on the outer surface of the flow domain. The various holes through the liner were then generated by deleting the corresponding cells. During the third stage the computational grid for the flow field outside the combustor was generated.

The passages of the swirler were not modelled, but only the outlets of the passages through the liner. In order to ensure that the correct mass and momentum fluxes were prescribed at the swirler outlets, the effective areas were only modelled. The holes in the cooling rings were modelled as rectangular holes with the same area as the effective round holes. Use was also made of discontinuous local grid refinement to model this fine detail. In the case of the primary, secondary and dilution holes, each hole was modelled using four cells. The annulus together with an outlet section present in the experimental rig was included, as shown in Figure 4.1. It was decided to include this outlet section as the pressure change which occurs in this section may also have a significant influence on the flow at the outlet plane of the combustor. A view of the final computational grid without the external flow field is shown in Figure 4.2.

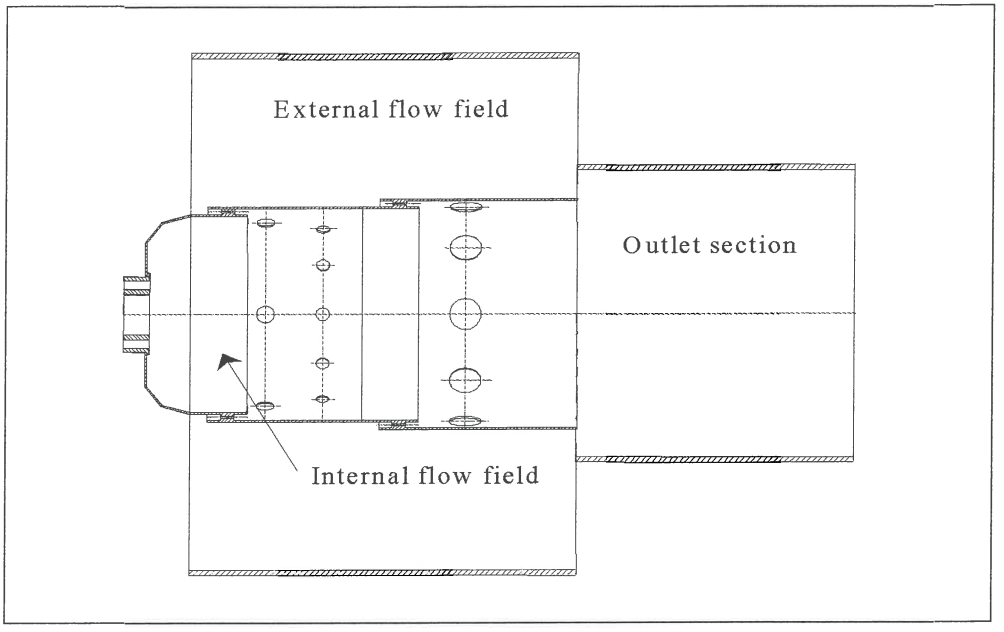

Figure 4.1 Computational domain chosen for the external and internal flow field

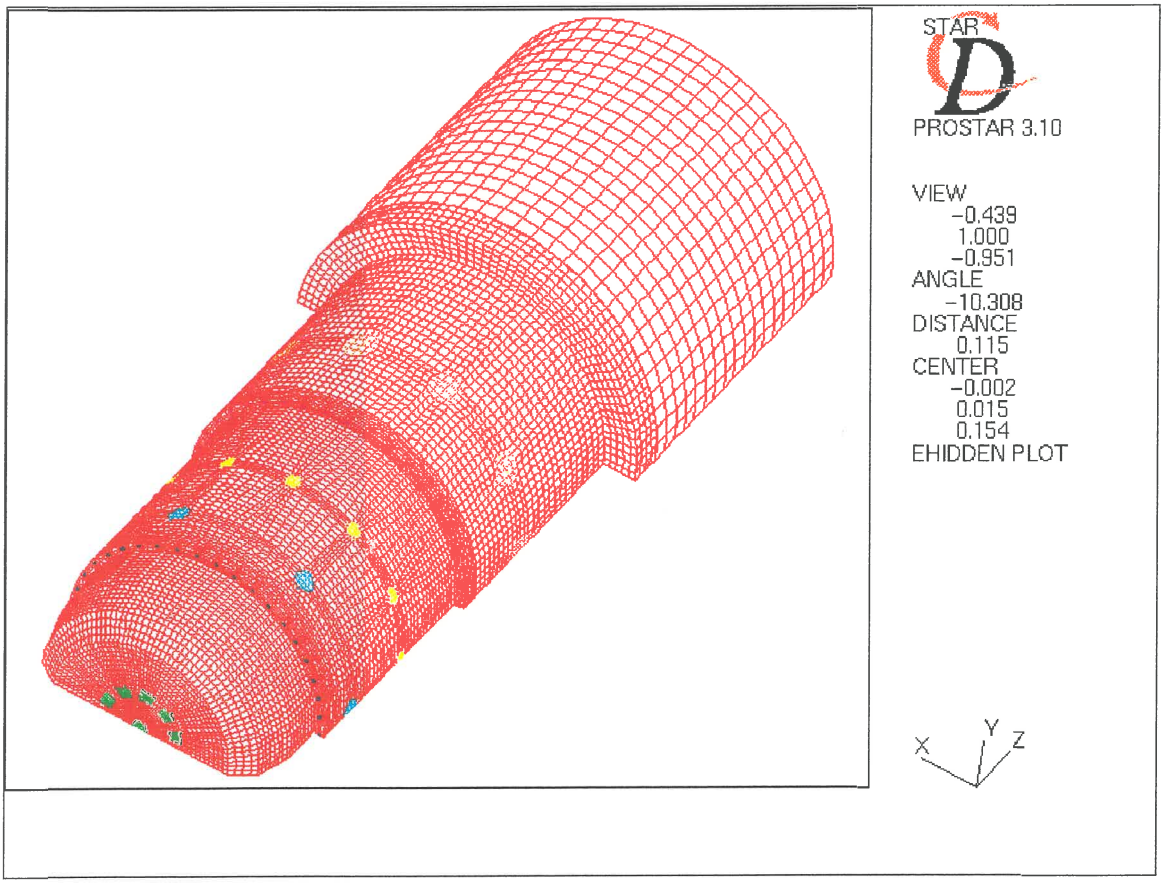

Figure 4.2 Computational grid used to model the internal flow field together with the outlet section

4.4 Boundary values

The boundary conditions prescribed consist of the conditions at the various inlets, the outlet, the symmetry plane and the inside and outside surfaces of the liner. The radial υ_r; tangential υ_θ; and axial υ_z velocities; the turbulence intensity I; mixing length L_e; temperature T and density ρ which were prescribed at the various inlets together with the operating conditions are summarized in Table 4.1 and Table 4.2.

Inlet	υ_r [$m.s^{-1}$]	υ_θ [$m.s^{-1}$]	υ_z [$m.s^{-1}$]	I	L_e [m]	T [K]	ρ [$kg.m^{-3}$]
Fuel	23.792	0	23.792	0	2.66×10^{-4}	293	1.679
Swirler	0	53.88	53.88	0.1	1.25×10^{-4}	300	1.011
Cooling I	0	0	78.415	0.1	2.82×10^{-5}	300	1.011
Primary	-67.756	0	39.338	0.1	1.97×10^{-4}	300	1.011
Secondary	-65.54	0	42.837	0.1	1.53×10^{-4}	300	1.011
Cooling II	0	0	78.868	0.1	2.82×10^{-5}	300	1.011
Dilution	-68.906	0	30.636	0.1	3.39×10^{-4}	300	1.011

Table 4.1 Boundary conditions at the various inlets

Air	
Patm [kPa]	88
ΔP_{comb} [kPa]	2.36
$T_{a,2}$ [K]	300
m_a [$kg.s^{-1}$]	0.1
Fuel	
T_f [K]	293
m_f [$g.s^{-1}$]	0.769

Table 4.2 Operating conditions used in the simulation

The velocity boundary conditions are obtained from the experimental discharge coefficient and jet angle. The basic equation for flow through a hole may be expressed as [30]:

$$\dot{m} = C_d A\sqrt{2\Delta P\rho} \tag{4.3}$$

By rearranging equation 4.3 the discharge coefficient is obtained in terms of the mass rate of flow:

$$C_d = \frac{\dot{m}}{A\sqrt{2\Delta P\rho}} \tag{4.4}$$

The jet angle is then calculated from the discharge coefficient:

$$\theta_j = \sin^{-1}\left[\frac{(K-1)}{(1.2C_dK)}\right] \tag{4.5}$$

Where K is the hole pressure-drop coefficient and is defined as:

$$K = \frac{\text{jet dynamic pressure}}{\text{annulus dynamic pressure}} = 1 + \frac{\Delta P_{comb}}{q_{an}} \tag{4.6}$$

The effective area by definition is:

$$A_{eff} = \frac{\dot{m}}{\sqrt{2\Delta P\rho}} = C_d A \tag{4.7}$$

The effective velocity at each inlet is then calculated from the mass rate of flow and density:

$$V_{eff} = \frac{\dot{m}}{\rho A_{eff}} \tag{4.8}$$

The radial, tangential and axial velocity component is lastly obtained from the effective velocity and jet angle:

$$v_{r,\theta,z} = V_{eff} \cos\theta_j \tag{4.9}$$

Because the turbulent character of the flow is dominated by the vigorous mixing which takes place inside the combustor, it has been found that the turbulence intensities prescribed at the inlets are not critical. The values for both the fuel mass fraction and the mixture fraction at the fuel were prescribed as 1.0, whilst the oxygen mass fraction and nitrogen mass fraction were respectively prescribed as 0.233 and 0.767 at all the other inlets. The liner was not included in the simulation and the walls were assumed to be adiabatic. Radiation was also not taken into account. At the outside surface of the liner a convective heat transfer boundary condition was prescribed. The ambient temperature was specified to be 300 Kelvin, whilst the effective heat transfer coefficient was taken to be 23.967 $W/m^2.K$. The upper and lower halves of the symmetry plane were defined as cyclic boundaries and all corresponding faces were integrally matched. Cyclic boundary conditions were prescribed for all variables on these faces. The assumption was made that due to the atomization process, the liquid fuel is introduced as a gas phase in the combustor. A more accurate representation would be to incorporate the Eulerian/Lagrangian two-phase model that looks at the interaction between a continuum gas phase and a discrete droplet phase.

4.5 Summary

Two of the most important aspects of CFD modelling in obtaining realistic predictions are the prescribed boundary conditions and magnitude of grid refinement. The grid density selected must be a balance between the requirement of modelling the geometry as accurately as possible, that the grid should be fine where steep gradients occur in the flow field and that the available computer resources should be able to cope with the problem. This, together with a judicious choice of boundary conditions, may lead to physically acceptable answers. This chapter provided a basic description of the CFD model that was employed to simulate combustion. A review of the combustion scheme, i.e. the PPDF-model implemented, was given and the computational grid and boundary conditions were examined.

CHAPTER 5

RESULTS AND EVALUATION

5.1 Preamble

The literature review identified the need for a numerical model that can simulate combustion in gas turbines. A research combustor that was designed with this purpose in mind was discussed. The physical properties involved during combustion was investigated experimentally and in chapter three the various measurements and geometrical positions that were recorded were described. In chapter four the numerical model implemented was discussed as well as the operating conditions that were simulated.

In this chapter the results obtained experimentally and numerically are presented. Experimentally, three different test conditions were investigated. These are discussed along with the test parameters that were used. From the results obtained, an evaluation is made of the efficiency of the combustor. Possible reasons are given for insufficient combustion as a result of chamber design. A direct comparison is also made between the experimental and numerical results. Discrepancies are pointed out and shortcomings of the experimental methods and/or numerical model are discussed.

5.2 Experimental results

5.2.1 Test parameters

The overall air-to-fuel ratio of the combustion chamber can vary between 20:1 and 150:1 depending on the type of engine. The test parameters used for the research combustor typically represents flying at altitude conditions. High overall air-to-fuel ratios were chosen to prevent damage to the liner wall that could be caused by an excessive heat load. Testing commenced under atmospheric conditions, the advantage being that the experimental setup is simplified as there is no need to preheat the inlet air, to obtain high pressures that are representative of the compressor outlet pressure, provide cooling of the fuel supply line, etc. The disadvantage of atmospheric test conditions is the inferior combustion efficiency that is obtained. However, when an evaluation is made between experimental results and a numerical model, the efficiency obtained can be discarded. The test parameters for the three different operating conditions used are presented in Table 5.1.

For all the test cases, the air mass flow rate was fixed and the amount of fuel varied to obtain different air-to-fuel ratios. As noted in chapter three, the combustor was theoretically designed to operate with an air flow rate of 0.1 $kg.s^{-1}$. The validity of this was assessed by obtaining measurements at various air flow rates. For values below 0.1 $kg.s^{-1}$ no significant variation in the temperature measurements were obtained, whilst values above the design point resulted in an increased pressure change across the combustor and increased turbulence intensity. The increase in turbulence intensity has a significant influence on the temperature field and as a result it was decided to keep the air mass flow rate fixed at 0.1 $kg.s^{-1}$. For reactive flow the pressure change across the combustor increased by 0.58 kPa compared to the cold flow analysis. This represents a total pressure change of 3.09 percent. It is assumed that the fuel temperature corresponds to ambient conditions, due to the relatively low fuel delivery pressure and mass flow rate.

Test case	**1**	**2**	**3**
Air/Fuel ratio	120	130	140
Ambient temperature [K]	290.15	289	288.65
Inflow pressure [kPa]	94	94	94
Inflow temperature [K]	309.45	304.55	301.05
Air flow rate [kg.s^{-1}]	0.1	0.1	0.1
Fuel flow rate [g.s^{-1}]	0.833	0.769	0.714
ΔP_{comb} [kPa]	2.92	2.89	2.89
P_{fuel} [kPa]	990	845	725
ρ_{air} [kg.m^{-3}]	1.0255	1.0424	1.0545
$\overline{T}_{exit}$ [K]	696.44	667.04	641.96
Equivalence ratio, ϕ	0.1226	0.1132	0.1051

Table 5.1 Test parameters and conditions

Preliminary CFD results predicted a maximum gas temperature of 2300 Kelvin inside the combustor. The maximum continuous working temperature that can be measured using an R-type thermocouple is equal to 1873 Kelvin. As a result it was decided to measure inside gas temperatures only at the highest air-to-fuel ratio for the different test cases. Each test case was repeated several times to assess the repeatability of the measurements. Except for slight variations due to atmospheric conditions, no significant changes in the measurements were recorded with repeatability measured within two percent. The hot junction of a thermocouple measures temperatures relative to a cold junction or reference temperature. Electrically controlled reference baths are often used which provide stable and uniform zones for the termination of thermocouple systems. These generally consist of a heated or cooled zone box thermostatically controlled to remain at a specified temperature [39]. Temperature measurements were obtained using ambient temperature as reference point. Ambient conditions however, varied and to compensate for this all the measurements recorded were adjusted to use 273.15 Kelvin as cold junction, and are therefore independent of these variations.

5.2.2 Inside gas temperatures

The inside gas temperatures were measured at five axial planes as discussed in chapter three. At an axial distance of 114.8 mm upstream of the exit plane a non-uniform temperature distribution exists as shown in Figure 5.1. The horizontal line corresponds to position one that has previously been defined. A hot section close to position one is evident, with an asymmetrical core region. From the temperature distribution alone it is difficult to account for the asymmetry present. This could however, be as a result of two factors: an uneven fuel spray distribution, or the amount of air that enters each primary jet and film cooling hole differs by a large extent. Due to the vigorous mixing process in the primary zone, the existence of "hot spots" in the primary zone efflux is often incurred, with the intermediate zone contributing to the amelioration of these [30].

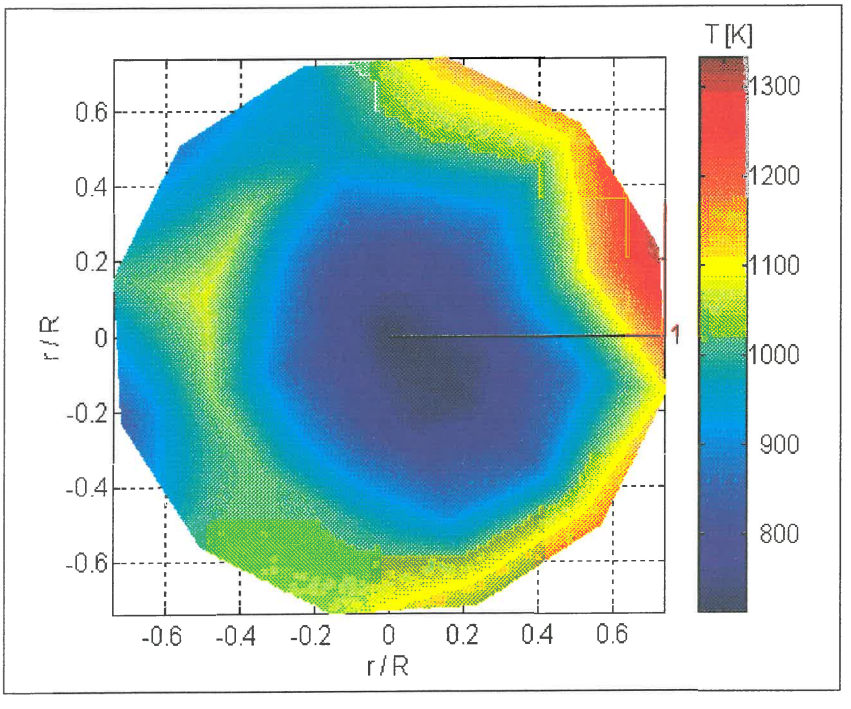

Figure 5.1 Inside gas temperature distribution at an axial distance of 114.8 mm from the combustor exit plane

A cold region in the centre characterizes the temperature field with the hot combustion products transported along the liner wall. The reason that the hot products are transported close to the liner is as a result of the sharp swirl angle that causes the reaction zones to form close to the wall. As the axial distance increases from the fuel inlet, the distribution becomes more symmetrical, with the cold region in the center expanding towards the liner wall as shown in Figure 5.2. The axial plane that corresponds to the dilution jet inlets, Figure 5.3 clearly shows the cooling effect of the dilution air entering into the combustion chamber. It should be noted that the angle of traverse for the measurements does not correspond to the angle of the various jets.

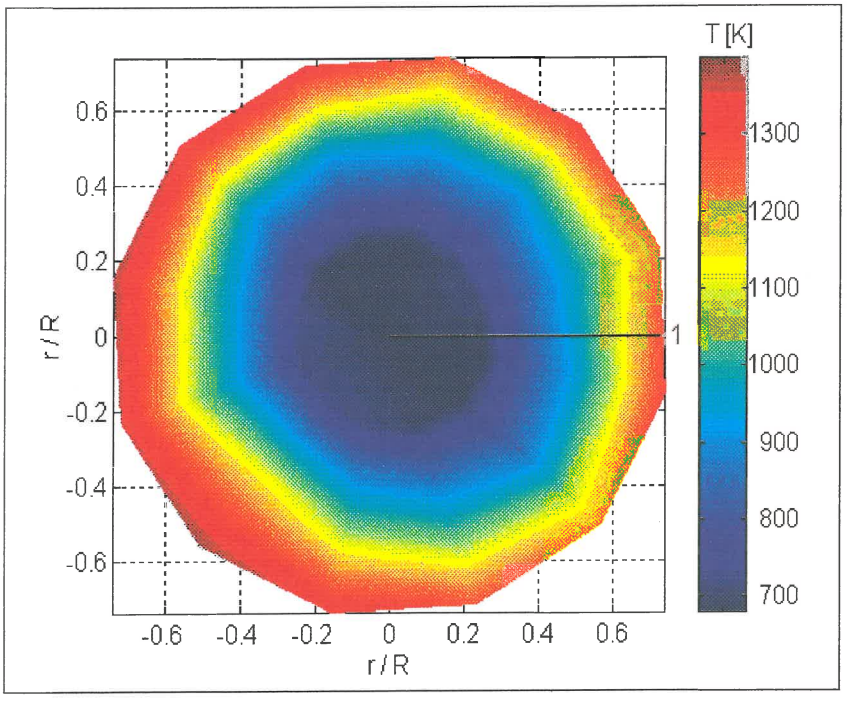

Figure 5.2 Inside gas temperature distribution at an axial distance of 89.8 mm from the combustor exit plane

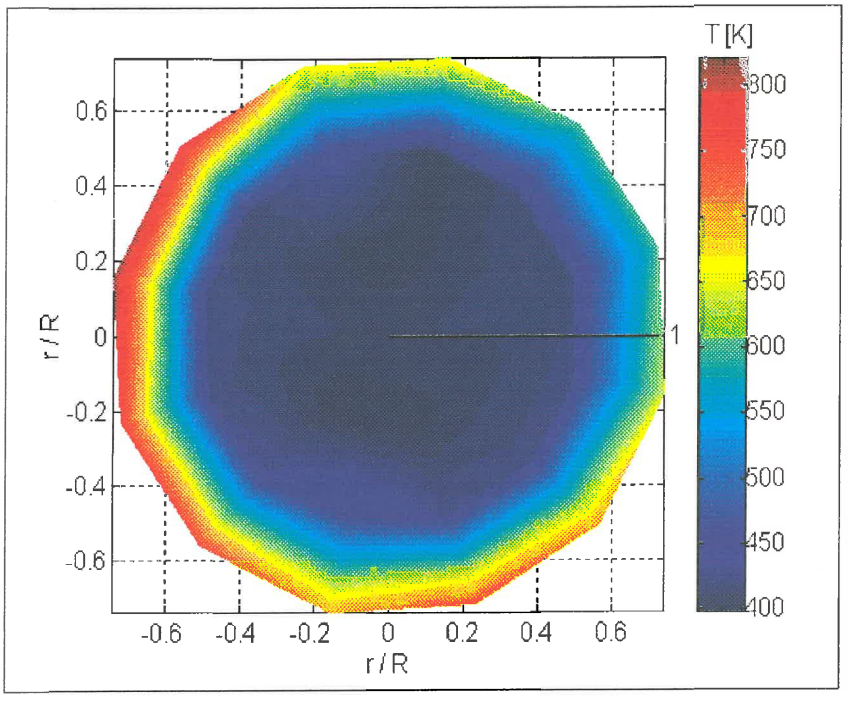

Figure 5.3 Inside gas temperature distribution at an axial distance of 39.8 mm from the combustor exit plane

Plotting the data on the geometrical symmetry plane of the combustor gives a better understanding of the temperature distribution (Figure 5.4 gives an interpretation to illustrate these results). Most of the fuel entering the combustion chamber is burned in the primary zone. This is as a result of the primary zone operating near stoichiometric conditions. It would therefore be expected that the maximum gas temperatures would occur in the primary zone. As more air is introduced through the secondary jets to provide an excess of oxygen to complete combustion, the gas temperatures will decrease from the primary to the secondary zone. The dilution air lowers the temperatures of the combustion products in the secondary zone before moving onto the turbine blades.

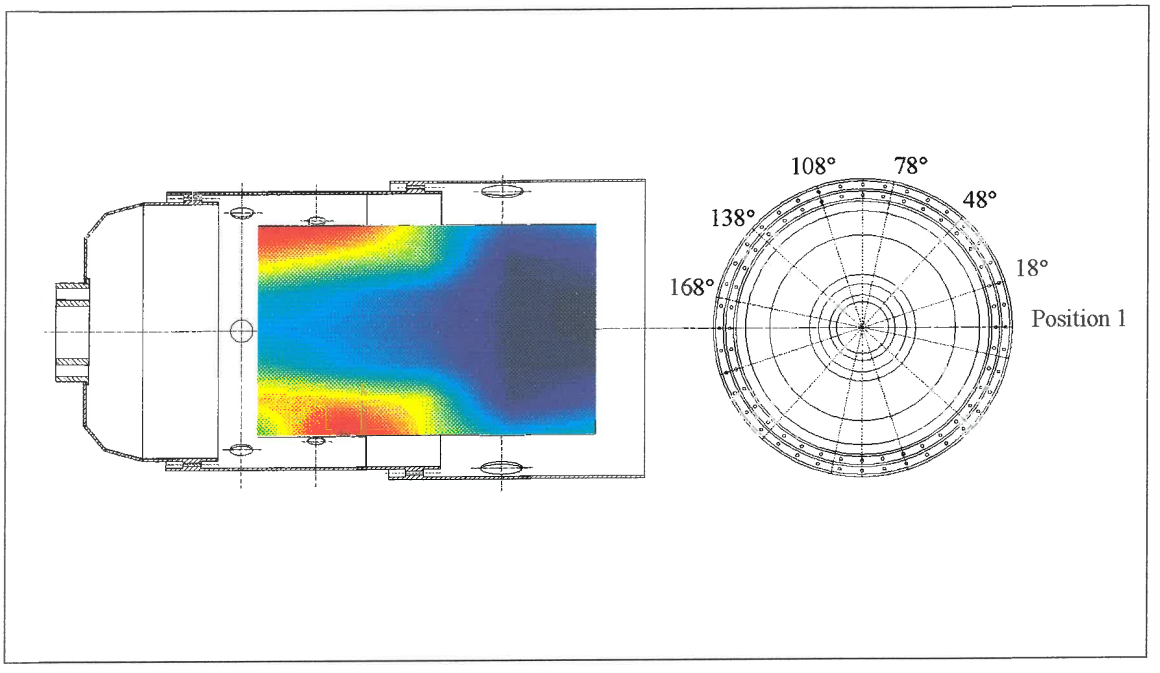

Figure 5.4 Interpretation of the temperature field inside the combustor at various angles from position one

From the measurements obtained in Figure 5.5 and Figure 5.6 it is observed that high temperatures occur close to the wall in the secondary zone. This indicates secondary combustion taking place as a result of incomplete combustion in the primary zone. The role of film cooling devices is to generate a protective film of cooling air between the wall and hot combustion gases. This cooling film, however, is gradually destroyed by turbulent mixing with the hot gas stream and as a result has a finite length of effectiveness. This may or may not include extension of the cooling film into the next cooling bay [40]. If combustion in the secondary zone takes place close to the wall, the cooling film will be destroyed. This will result in an increase of liner temperatures in the secondary zone. During testing this was noticed visually inside the combustor, with overheated sections in the intermediate zone compared to the rest of the liner. The inlet air from the dilution jets results in the formation of a low temperature area close to the exit of the combustor. To ensure a satisfactory temperature profile at the chamber outlet, there must be adequate penetration of the dilution air jets, coupled with the correct number of jets to form sufficient localized mixing regions. If the total dilution-hole area is spread over a large number of small holes, penetration will be inadequate, and a hot

core will persist through the dilution zone. At the other extreme, the use of a small number of large holes will result in a cold core, due to overpenetration, and unsatisfactory mixing [30]. The latter applies to the research combustor with most of the dilution air flowing along the center of the combustor, and consequently mixing with the combustion products is inadequate.

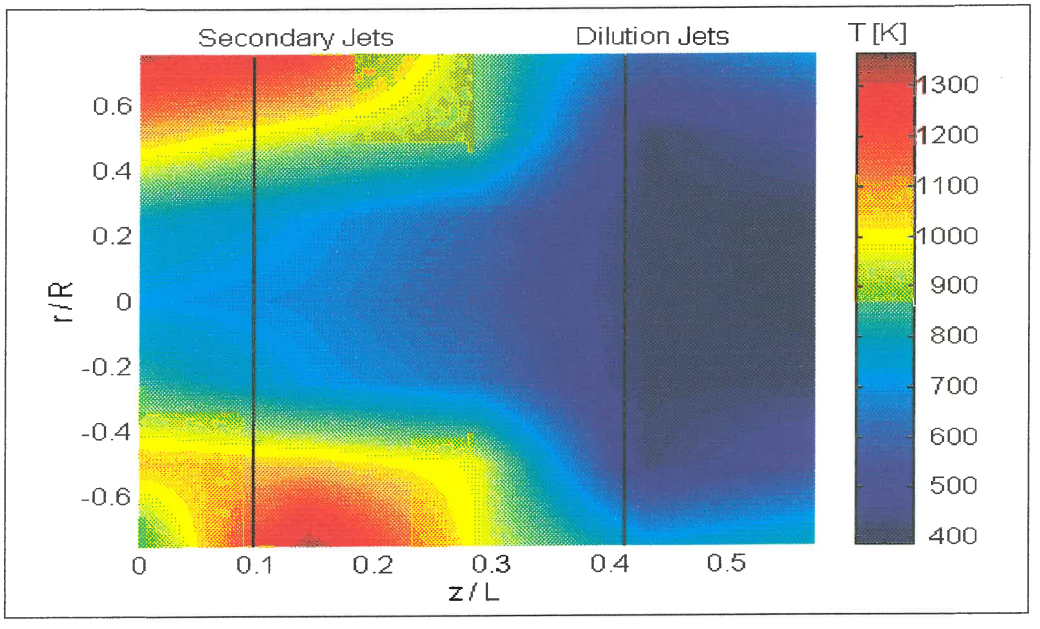

Figure 5.5 Inside gas temperature distribution at an angle of 18-degrees from position one

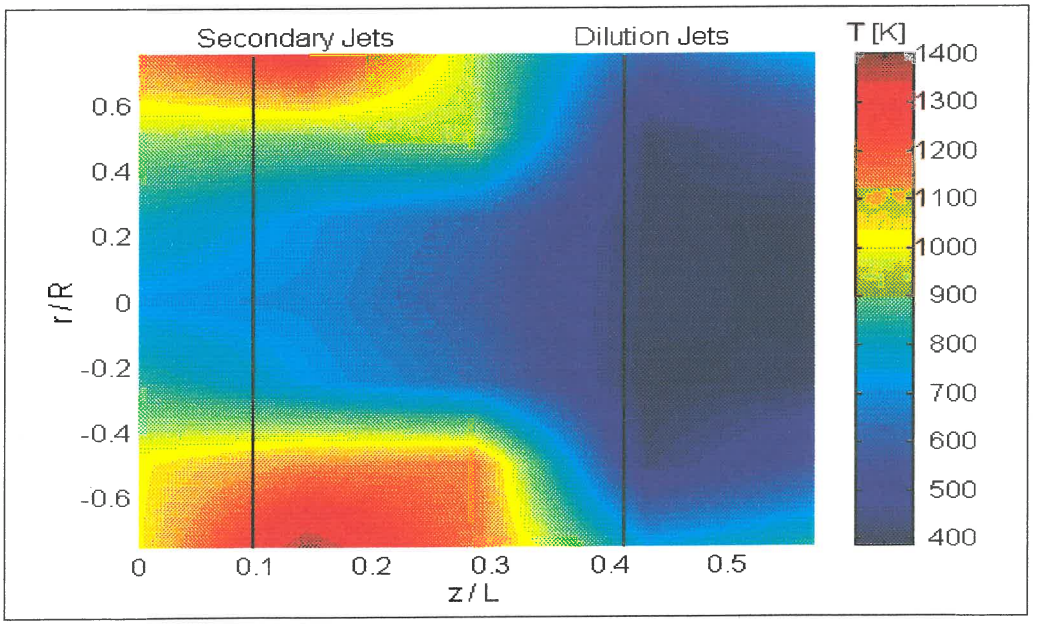

Figure 5.6 Inside gas temperature distribution at an angle of 48-degrees from position one

5.2.3 Liner wall temperatures

The outer liner wall temperatures for an air-to-fuel ratio of 130 is shown in Figure 5.7. The highest liner temperature was recorded in the secondary zone. This confirms the measurements acquired from the inside gas temperatures that indicate combustion close to the wall in this section. The liner temperatures decrease from the secondary zone axially along the combustor to a minimum in the dilution zone. A maximum temperature difference of 12-percent was measured circumferentially at the four positions that coincided with one another at an axial distance. No large thermal gradients therefore exist between these positions. The increase in average circumferential temperature with air-to-fuel ratio is pointed out in Figure 5.8.

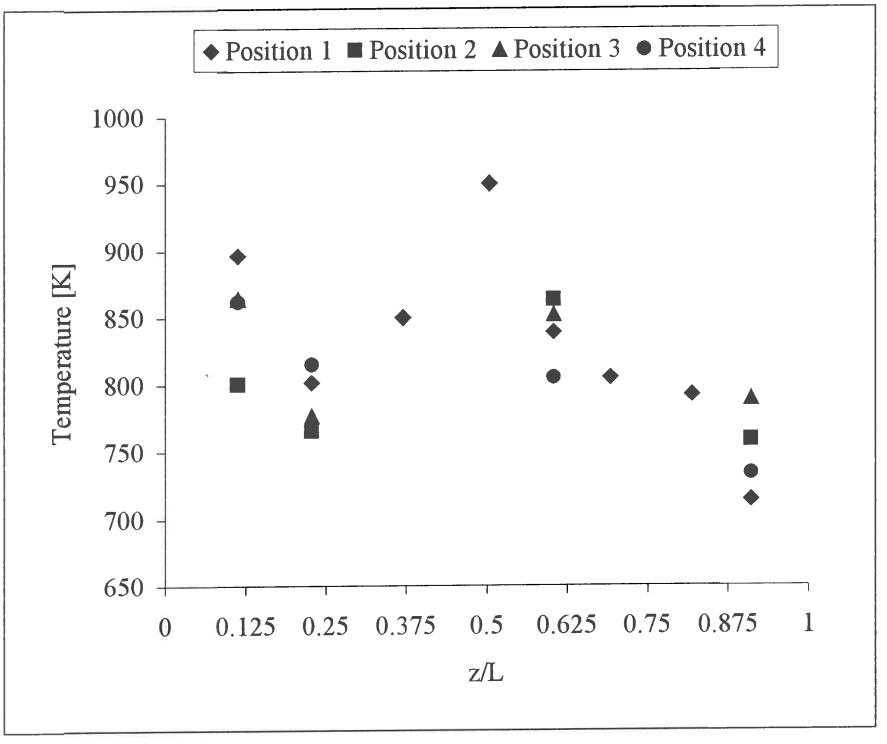

Figure 5.7 Combustor liner wall temperatures for AFR=130

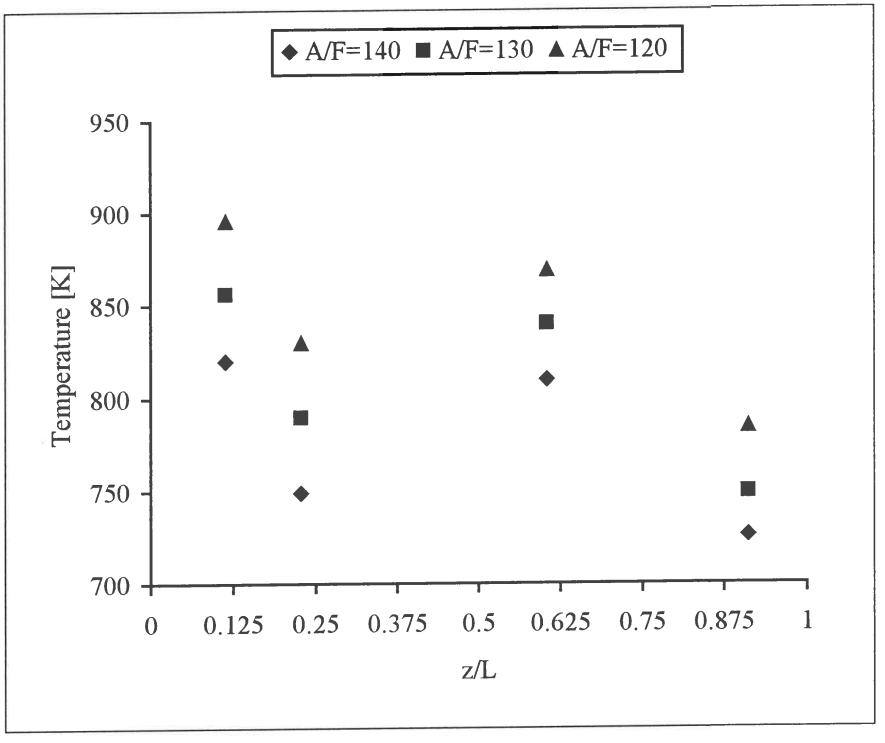

Figure 5.8 Average circumferential liner temperature for different AFR's

5.2.4 Exit gas temperatures

As noted in chapter two, the distribution of exit gas temperatures is an important parameter in the design of turbine blades. Shown in Figure 5.9 is the distribution of exit gas temperatures for an air-to-fuel ratio of 130. As expected from the inside gas temperatures that were recorded the distribution is characterized by the cold core formed by the dilution air. Ideally, a symmetrical span profile must exist to prevent the formation of hot sections downstream from the combustor. Evident from the measurements is the asymmetry, mainly formed by the colder region between positions four and one. Referring to the liner temperatures measured at an axial distance of z/L=0.9113 the minimum temperatures were recorded at positions one and four and confirm the distribution of exit gas temperatures.

In practice it is very unlikely that a uniform profile will be obtained, as there is not enough time available for good mixing to take place. The shielded thermocouples were mounted in several different ways on the traverse mechanism in an effort to reduce the amount of asymmetry. The precision with which the fuel inlet is mounted relative to the centre line of the combustion chamber is fixed and the only parameter that can be changed is the fuel injector. Irrespective of these changes the same temperature distribution was obtained, indicating that the asymmetry can be contributed to the mechanical construction of the combustor. The constant hot and cold cycles experienced during testing also has a significant influence on the geometrical form of the chamber.

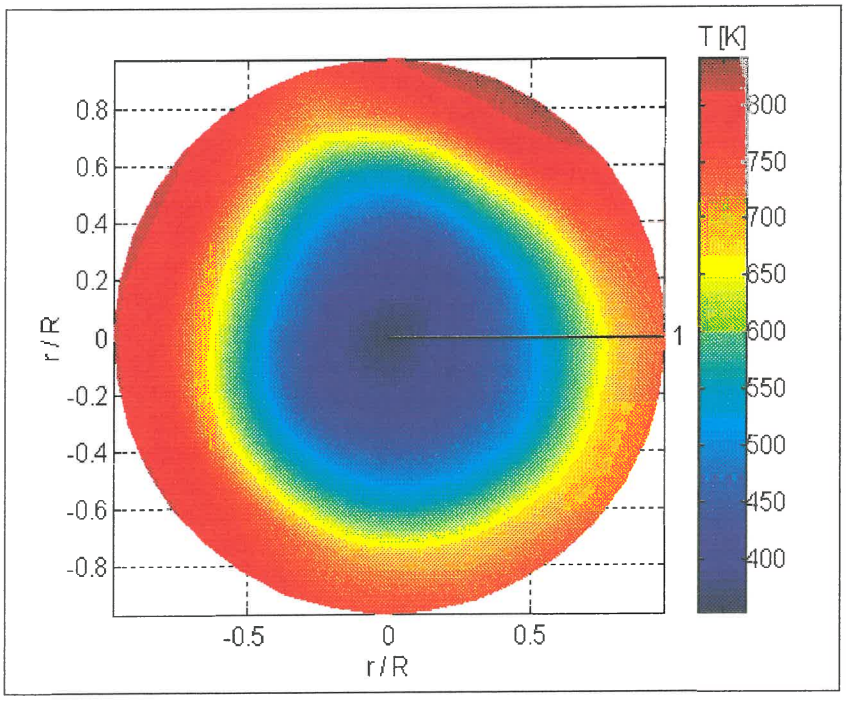

Figure 5.9 Exit gas temperature distribution for AFR=130

The linear decrease in average exit temperature - obtained from the mass-flow-weighted mean of all exit temperatures - with an increase in air-to-fuel ratio, is shown in Figure 5.10. Increasing the air-to-fuel ratio results in an overall temperature decrease, a higher pattern factor and a decrease in efficiency.

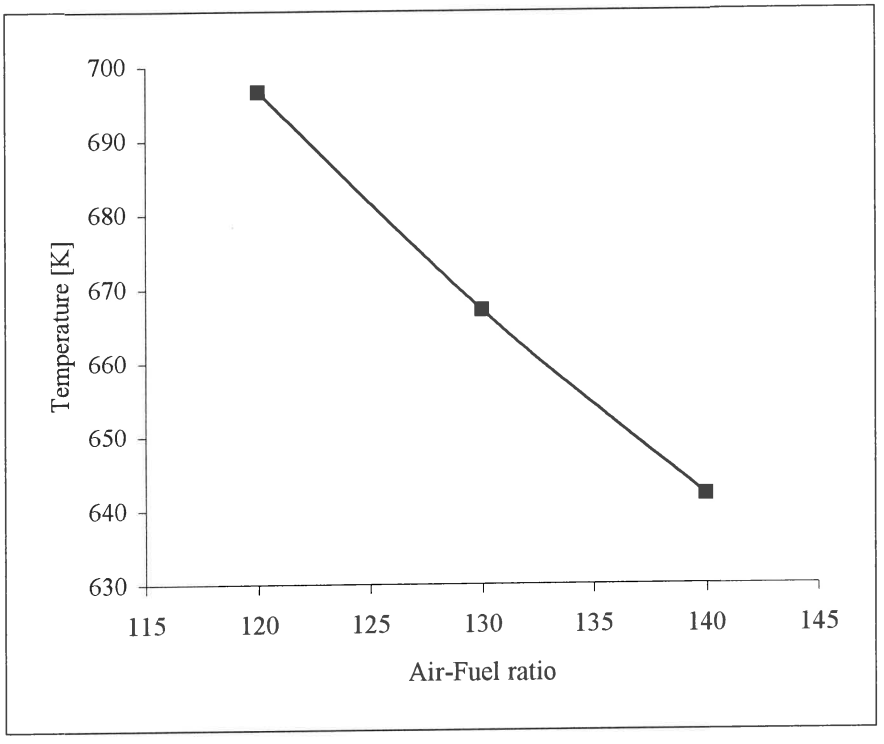

Figure 5.10 Average exit gas temperature for different AFR's

5.3 Numerical results

One of the major advantages of CFD is the ability to provide detailed insight and comprehensive information that is not always possible to obtain from experimental measurements. The distribution of velocity magnitudes on the geometrical symmetry plane obtained from the numerical simulation of the research combustor is shown in Figures 5.11-5.12. The highest velocities are procured at the swirler and various jet inlets. The recirculating low velocity area in the primary zone that is formed by the interaction of the inlet air from the swirler and primary jets are overt. It is arranged that the conical

fuel spray from the burner intersects the recirculation vortex at its center. This action, together with the general turbulence in the primary zone, greatly assists in breaking up the fuel and mixing it with the incoming air [41]. The air entering the primary jets has an increased penetration depth compared to the secondary and dilution air. The reason is twofold, firstly the primary hole area is smaller in relation to the dilution holes and secondly the inlet air from the secondary and dilution holes are diverted by the combustion products flowing along the core. A larger recirculating region that is formed between the primary and secondary jets is clearly visible.

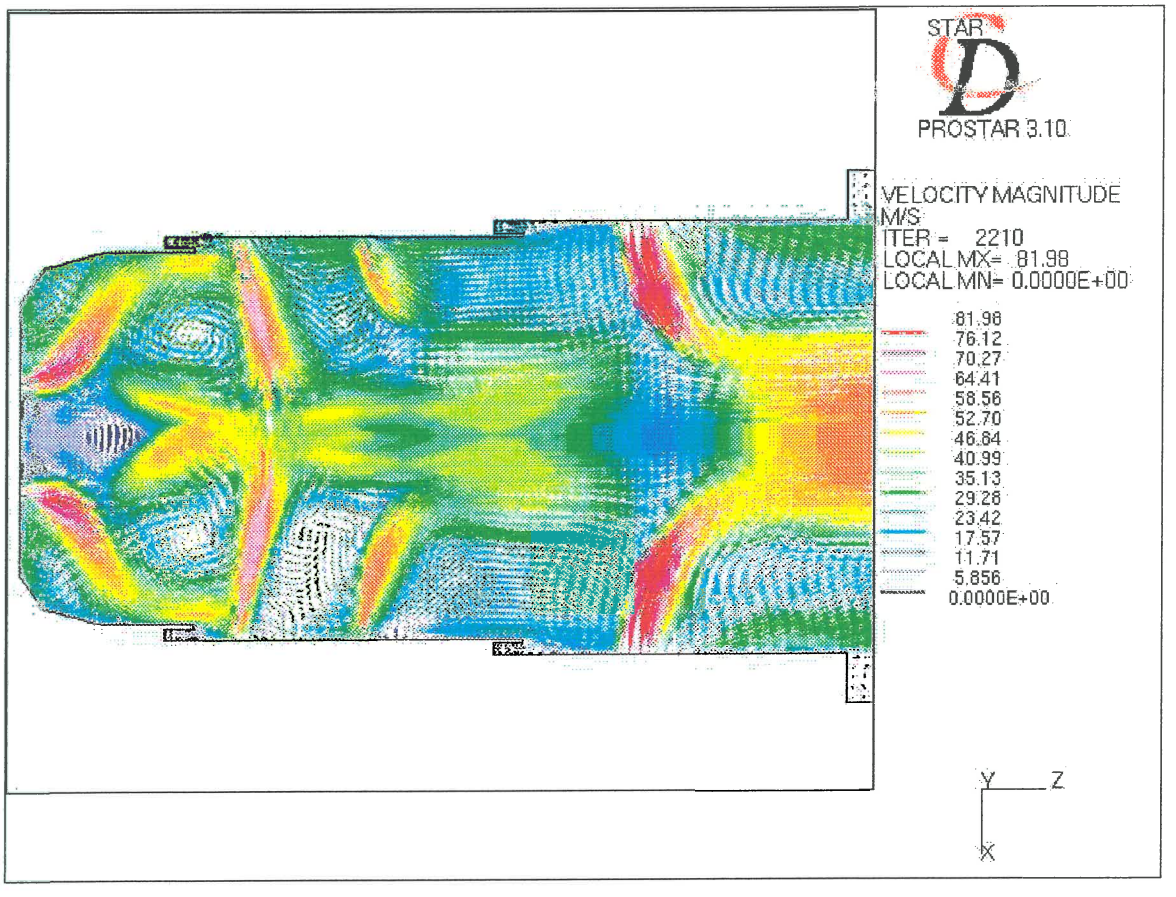

Figure 5.11 Velocity vectors depicting the flow field inside the research combustor

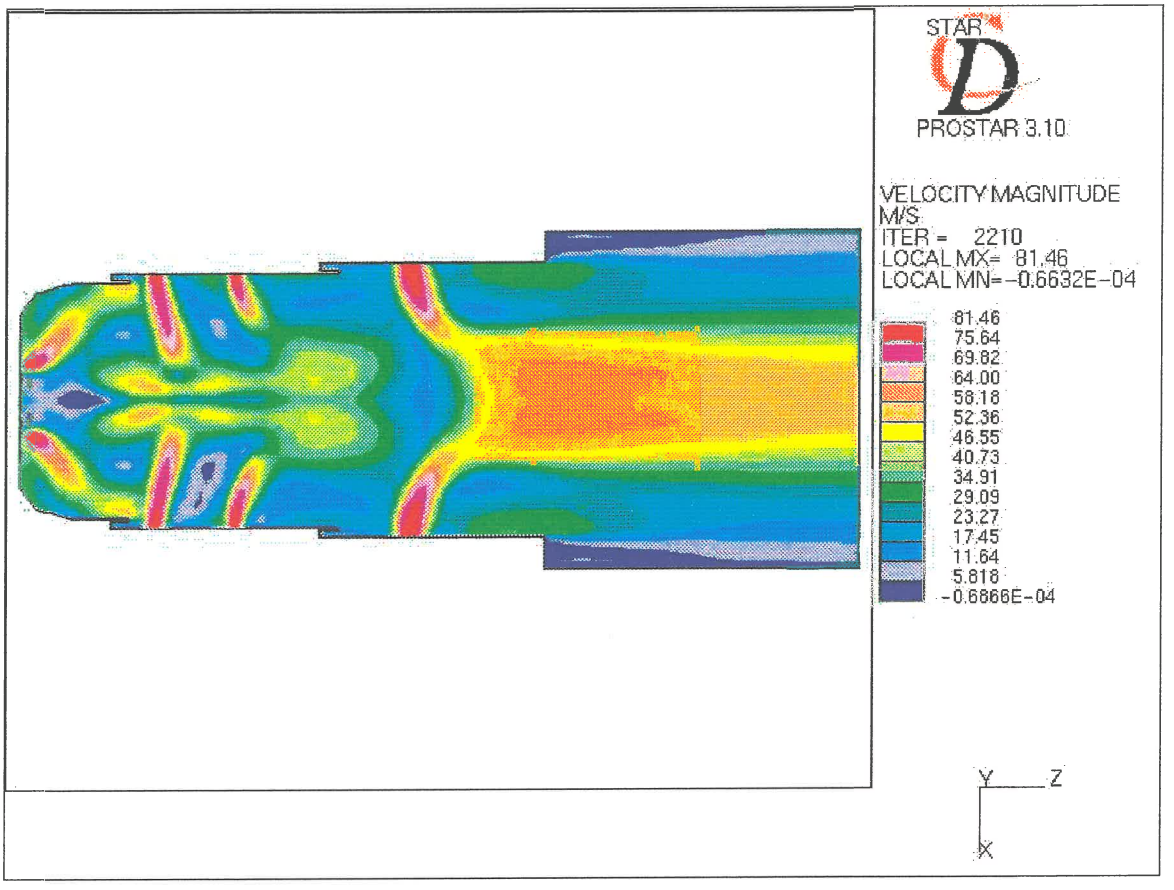

Figure 5.12 Velocity magnitudes depicting the flow field inside the research combustor

The temperature distribution on the geometrical symmetry plane of the combustor is presented in Figure 5.13. A maximum temperature of 2160 Kelvin is predicted, with high temperatures appearing in the primary and secondary zone close to the liner wall. The lowest temperatures are predicted in the dilution zone and along the centre of the combustor. The hot sections between the primary and secondary jets, as well as after the secondary jets indicate that the combustion products penetrate between the jets, and that combustion occurs in the intermediate zone. Significant from the results is the inability of the film cooling air to provide a protective cooling layer between hot combustion products and the inner liner wall. From the velocity field it is noted that the film cooling air proceeds a short distance from the inlets before being halted by the hot gases flowing downstream.

.

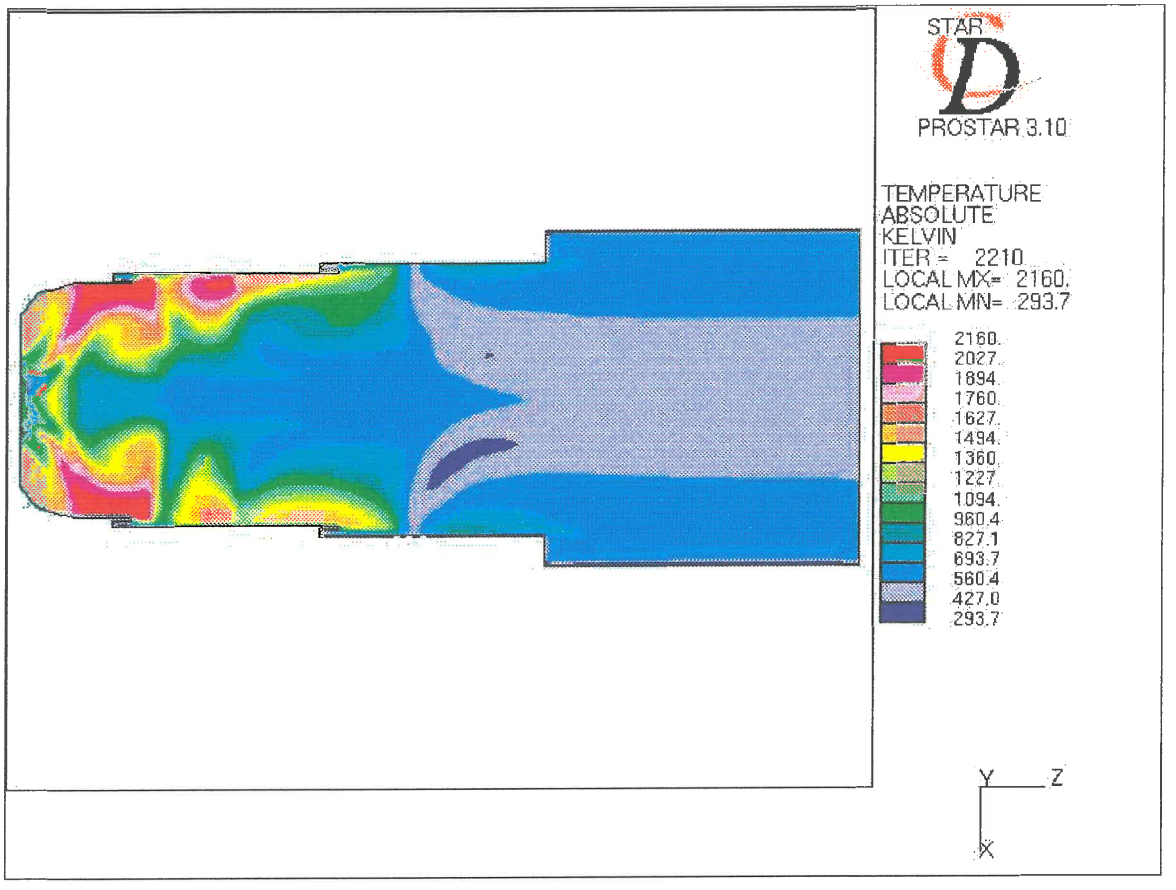

Figure 5.13 Temperature field inside the combustor on the geometrical symmetry plane

At the exit of the combustor the gas temperatures decrease from the outside to the inside and then increases again at the center of the combustor as shown in Figure 5.14. An interesting pattern is observed in the temperature contours on the outlet plane. The hot sections that occur along the perimeter are in line with the dilution holes and are an indication of how the hot gases which are squeezed between the air entering the dilution jets, curl around them.

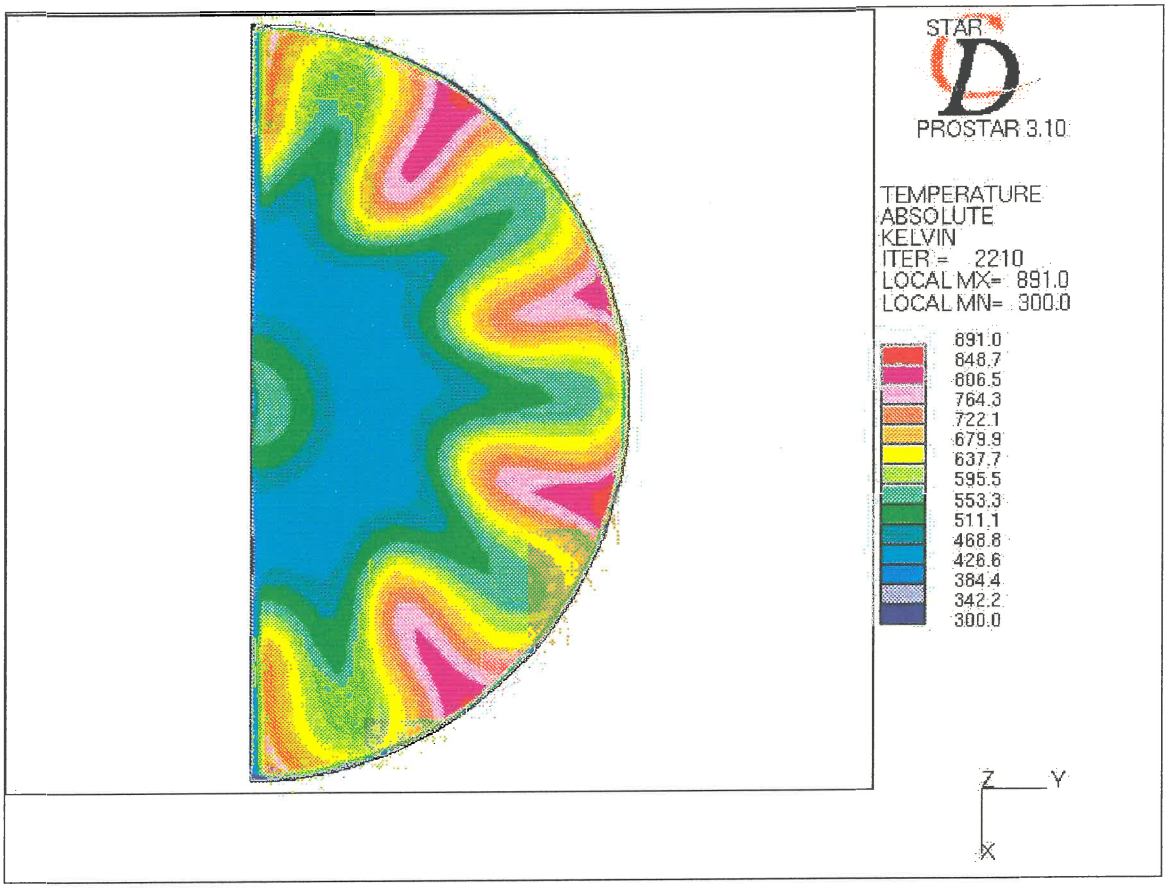

Figure 5.14 One-half of the symmetrical gas temperature distribution at the exit plane of the combustor

5.4 Evaluation

Experimental and numerical results indicate that temperatures increasing from the centre to the liner wall delineate the temperature field inside the combustor. Incomplete combustion occurs in the primary zone, reducing the overall combustion efficiency. Although no velocity measurements were obtained to determine the shape and size of the recirculation region, the velocity distribution from the numerical results indicate that the amount of air entering through the swirler and primary jets results in recirculation zones that are not fully optimized. Cameron et al [7] note that the common perception of the flow field in a gas turbine combustor is the presence of an on-axis recirculation zone produced as a result of the interaction between the swirl air and the primary jet flow. It

was found that by increasing the swirl air, the recirculation zone was transformed into an on-axis configuration. In contrast to this, a condition was not found for which the primary jet flow played a role in enhancing the recirculation zone strength or size. The isothermal amount of air entering the research combustor through the swirler consists of 8.25 percent of the total air mass flow. This amount is fairly low compared with quantities that vary between 18 and 45 percent depending on the type of combustor [41,7]. By increasing the amount of swirl air it would be possible to increase combustion efficiency in the primary zone and reduce the liner temperatures in the secondary zone.

It is also evident that the incorrect flow splits exist at the various film cooling and dilution holes. In general, the lower the amount of air employed in film cooling, particularly in the primary zone, the better the prospect is of achieving 100% combustion efficiency at the chamber outlet [30]. Despite this possible increase in combustion efficiency it was found that the amount of film cooling air employed does not provide sufficient cooling of the inner liner wall. The amount of air entering the first and second film cooling slots are 1.73 and 1.74 percent respectively. On modern combustors, up to 50 percent of the total air-mass flow is employed in liner wall cooling [30]. The numerical results indicate that the film cooling air is almost non-existent as turbulent mixing with the hot gas stream destroys it. By increasing this amount of air, the liner temperatures in the secondary and dilution zone will decrease, and it would be possible to test at lower air-to-fuel ratios that is representative of ground idle and take-off conditions. In contrast to this, the quantity of dilution air must be reduced to optimize mixing with the combustion products. The temperature contours at the exit plane point out that the dilution air flows along the center with the combustion products on the outside. Sufficient mixing must exist between hot gases and dilution air to prevent the formation of hot sections downstream of the combustor.

A direct comparison between the experimental and numerical results shows that the CFD model overpredicts the magnitude of temperatures in certain areas. Along the core and in the dilution zone, the temperatures are in close proximity. However, the maximum

temperatures in the primary and secondary zone close to the liner wall are overpredicted. These differences are mostly related to the numerical model:

- The assumption of adiabatic walls, that is, no heat transfer is invalid. The annulus on the test rig was not insulated and although the magnitude is not directly as a consequence of convective heat transfer, wall temperatures of 400 Kelvin were measured on the outside of the annulus. In the case of adiabatic walls all the heat is assimilated by the annuli flow which in return is transported into the combustion chamber increasing gas and liner temperatures.
- An asymmetry is present in the velocity and temperature field obtained numerically. The assumption to model only half of the combustor is therefore questionable and whether the symmetry plane of a swirling combustion process is at the same position as the geometrical symmetry plane.
- Radiation was not included in the simulation. Although this would result in an increased heat transfer to the gas particles and liner wall, radiation does not have a predominant influence at high air-to-fuel ratios. It is also important to account for radiation losses incurred experimentally as well as on the outside of the flame tube.
- The numerical model does not adequately model the geometrical aspects of the research combustor. The swirler forms an important part in the combustion process and is not included in the model. Although the computational effort is increased it is necessary to model the geometries as accurate as possible to obtain realistic predictions.
- Liquid fuel was used during experimental testing. The assumption is made that due to atomization, the fuel is introduced into the combustor in a gas phase. However, two-phase flow is present consisting of a gas phase and small fuel droplets following different trajectories. In spray combustion systems, an accurate representation of the fuel droplets is often considered important [13].
- The fuel nozzle was not geometrically modelled. At the inlet an angle of fuel spray was prescribed. However, the fuel spray embodies a conical shape filled with a liquid and gas phase and by specifying an angle all the fuel is directed into a single area, which is incorrect.

The experimental and numerical distribution of temperatures at the exit plane of the combustor is in good agreement. Except for an increase in temperatures at the center - which can be related to the boundary conditions prescribed - the numerical model is capable of predicting the correct magnitudes and distributions. As noted in chapter one, a direct comparison of liner wall temperatures is difficult. The reason being that a small difference in probe position can make all the difference between recording and failing to record a "hot spot". The measured wall temperatures are therefore very useful in substantiating trends and measurements obtained inside the combustor, but care must be taken when it is used for direct comparison with numerical results.

Despite the inadequacies of the CFD model it is promising to observe the numerical model being capable of capturing the temperature distribution and trends obtained experimentally. This sustains the potential of finite difference techniques in modelling gas turbine combustors. With the ever-increasing computing capabilities, CFD models should be able to predict the different physical properties within an acceptable limit.

5.5 Summary

This chapter provided and discussed the results obtained experimentally and numerically. Experimental results were obtained for different test conditions and a numerical model was validated against these. It was found that inferior combustion efficiency exists, due to the incorrect air flow splits at the various inlets. The numerical model overpredicted the magnitude of temperatures, but was able to capture the distribution of the temperature field. The shortcomings of the numerical model and assumptions made were pointed out.

CHAPTER 6

SUMMARY, CONCLUSIONS AND RECOMMENDATIONS

6.1 Summary

The turbulent, swirling flow field in a gas turbine combustor is complex and difficult to analyze. Although showing potential, numerical models predicting the physical elements of the turbulent flow field still needs further development. Most of the current models are capable of capturing the correct trends and distributions, but not the magnitudes of the various properties. Therefore, CFD is rather used as an aid in the design process to assess the influence of different design changes and not as primary design tool. Consequently, costly and timely experimental investigations are necessary to measure the performance of a combustor.

Complex geometries and challenging operating conditions have resulted in a limited number of experimental investigations and measurements that can be used for validation purposes. Most research done dates back to the previous decade, focusing on combustors with simple geometries that do not provide a sufficient challenge to present-day computing capabilities. In this study, the need was addressed to obtain detailed experimental measurements that capture the three-dimensional thermal field inside a research combustor. A description of the research combustor was given, illustrating the various features that are representative of practical combustors. All possible

measurements, i.e. inside gas, liner wall and exit gas temperatures were recorded for different air-to-fuel ratios. Due to the experimental setup and test conditions that were used, inside gas temperatures - which were inadequately investigated and/or precluded by other researchers - were measured successfully. The experimental results recorded were presented and discussed in detail.

Using a commercially available code, a numerical model was developed to simulate the research combustor and test conditions used during the experimental investigation. A description of the combustion scheme, i.e. presumed-PDF model of unpremixed turbulent reaction was given. The computational grid and boundary conditions implemented in any numerical model are important and form the basis of obtaining realistic predictions. Each of these were examined and the shortcomings of the computational model were highlighted. A comparison between the experimental and numerical results showed that the gas temperatures are overpredicted. This can be related to the boundary conditions that were prescribed. However, the model was capable of capturing the correct distribution of temperatures and trends obtained experimentally. This points out the potential of CFD and the need for further development.

Important conclusions drawn from the research done, as well as contributions, are presented in the subsequent section. Further developments, both experimental and numerical are needed and recommendations for further research provide an apt ending to this study.

6.2 Conclusions and contributions

The main conclusions and contributions reached during the course of the study can be summarized as follows:

- Numerical models developed to simulate gas turbine combustion, have to be validated against experimental data. An experimental investigation was done that captured the thermal field of a can-type combustor for this purpose. Inside gas, liner wall and exit gas temperatures were measured successfully.

- Experimental results showed that incomplete combustion occurs in the primary zone, thereby reducing the overall efficiency. The numerical results confirmed this, indicating that the recirculation zones that are formed in the primary zone are not fully optimized. Unburnt fuel is transported into the intermediate zone where secondary combustion occurs. As a result the liner temperatures in this section increase and the measured wall temperatures reflect this.

- Also evident from the results are the incorrect flow splits at the various inlets. The amount of swirling air dominates the size and strength of the recirculation zone. This amount must be increased to reduce the inefficiency as a result of the latter conclusion that was reached. The amount of dilution air must be reduced to prevent overpenetration and insufficient mixing with the hot combustion products, as was found from the experimental and numerical results. It is also concluded that the film cooling air is almost non-existent and does not provide a sufficient layer of cooling air between the hot gases and inner liner wall.

- The numerical model overpredicts the gas temperatures inside the combustor. This is directly related to the shortcomings and assumptions made in the development of the computational model. The discrepancies can be summarized as: single-phase flow, no radiation, adiabatic walls, symmetry and geometrical features not modelled. Despite these shortcomings, trends and distributions obtained experimentally were predicted correctly. The numerical model is capable of providing detailed insight and comprehensive information that is not always possible to obtain from experimental measurements. The present CFD model needs further development to utilize the available resources and potential to accurately predict combustion properties.

6.3 Recommendations for further work

Recommendations for further work, applicable to the present study can be summarized as follows:

- In this study, only the temperature field was investigated experimentally. Further experimental work must include velocities and species concentrations. A first approximation can consist of the velocity field during isothermal conditions, reducing the experimental effort and instrumentation needed to conventional measurement methods.

- An experimental investigation that determines the influence of different design changes and operating conditions on combustor performance is needed. Some of these changes include the amount of swirl air, swirl angle, preheated and pressurized inlet air, fuel type, fuel spray angle, increased film cooling air and measurements at lower air-to-fuel ratios. Investigating these changes will result in the expansion of the current experimental database.

- Improvement of the current numerical model is needed. The shortcomings of the model, as discussed in the previous section must be investigated. Modelling must couple the external and internal flow field, reducing the inlet boundary conditions that are prescribed to velocities and pressures at the compressor outlet. Two-phase flow must also be incorporated into the combustion scheme and the fuel nozzle must be modelled to obtain a realistic distribution of the fuel entering into the combustion chamber.